Cascade Annealing of Tungsten Implanted with 5 keV Noble Gas Atoms

Kolk, G.J. van der; Veen, A. van; Caspers, L.M.; De Hosson, J.T.M.

Published in:
Nuclear Instruments and Methods in Physics Research Section B%3A Beam Interactions with Materials an

DOI:
10.1016/0168-583X(84)90298-2

Nuclear Instruments and Methods in Physics Research B2 (1984) 710–714
North-Holland, Amsterdam

CASCADE ANNEALING OF TUNGSTEN IMPLANTED WITH 5 keV NOBLE GAS ATOMS: A COMPUTER SIMULATION

G.J. VAN DER KOLK, A. VAN VEEN and L.M. CASPERS

Delft University of Technology/Interuniversity Reactor Institute, Mekelweg 15, 2629 JB Delft, The Netherlands

J.Th.M. DE HOSSON

Materials Science Centre, Nijenborgh 18, 9747 AG Groningen, The Netherlands

The trapping of vacancies by implanted atoms is calculated. After low energy implantation (5 keV) of tungsten with heavy noble gas atoms most of the implanted atoms are in substitutional position with one or two vacancies closer than two lattice units. Under the influence of the lattice distortion around the implanted atoms the vacancies follow a preferential migration path towards the implant during annealing. With lattice relaxation simulations migration energies close to the implanted atom are calculated. Monte Carlo theory is applied to obtain trapping probabilities as a function of implant–vacancy separation and temperature. An estimate of the initial implant–vacancy separation follows from collision cascade calculations. The results show that nearby vacancies are trapped by the implanted atoms.

1. Introduction

After implantation of tungsten with heavy noble gas atoms it is found that there is a recovery step which can be attributed to vacancy mobility and subsequent recovery at the surface (stage III). With thermal helium desorption spectrometry (THDS) it is also seen that in stage III a defect-complex is formed probably consisting of a substitutional noble gas atom and one or more extra vacancies. Upon further annealing these defect complexes dissociate. For some implants it was shown that the defects formed then are substitutional noble gas atoms [1].

Recently performed perturbed angular correlation experiments (PAC) in which tungsten was implanted with 25 keV Ag and In, revealed a near 100% substitutionality of the implant immediately after implantation, whereas with THDS substitutionality of the implant was seen only after annealing above stage III [2].

The aim of this study is to show the presence of near-vacancies at the implant after implantation. Those near vacancies will make it impossible for THDS to detect the implanted atoms. Furthermore it will be shown that during annealing a large fraction of these near vacancies will migrate to the implant. Migration energies near the implanted atoms are estimated using the short-range pair-potential calculations. The thus obtained migration energies are used in a Monte Carlo program to calculate the vacancy capture radius for a uniform vacancy distribution and to calculate trapping probabilities for vacancies on sites within 8 lattice units (LU) from the implant. An estimate of the initial implant–vacancy separation follows from collision cascade simulations with MARLOWE [3].

2. Static lattice calculations

In the static lattice calculations a small crystallite of $17 \times 17 \times 17$ atoms containing a defect in the centre relaxes to a minimum energy configuration. The vacancy migration energies were found by calculation of the total energy of the relaxed crystallite with a lattice atom in a fixed position between two vacancies. The results obtained with this method depend on the set of pair-potentials applied. In this study the widely-used Johnson–Wilson short-range W–W potential was taken. It should be realized that the migration energy calculated with this potential is about 0.4 eV too low [4,5]. Since our interest is the relative preference for certain directions in a strained crystal this does not affect our calculations. The tungsten–noble gas potentials were calculated by Baskes [6] applying the Hartree–Fock method. It was found that there are two equivalent barriers for a jump in the (111) direction, formed by the two triangles of atoms in a (111) plane through which the moving atom has to migrate. Calculated vacancy migration energies around substitutional noble gas atoms are shown beside the arrows of the so-called transition matrices in fig. 1. The encircled number in the box indicates which neighbouring position is concerned; 1 is the nearest neighbour. The transition matrices are simi-

0168-583X/84/$03.00

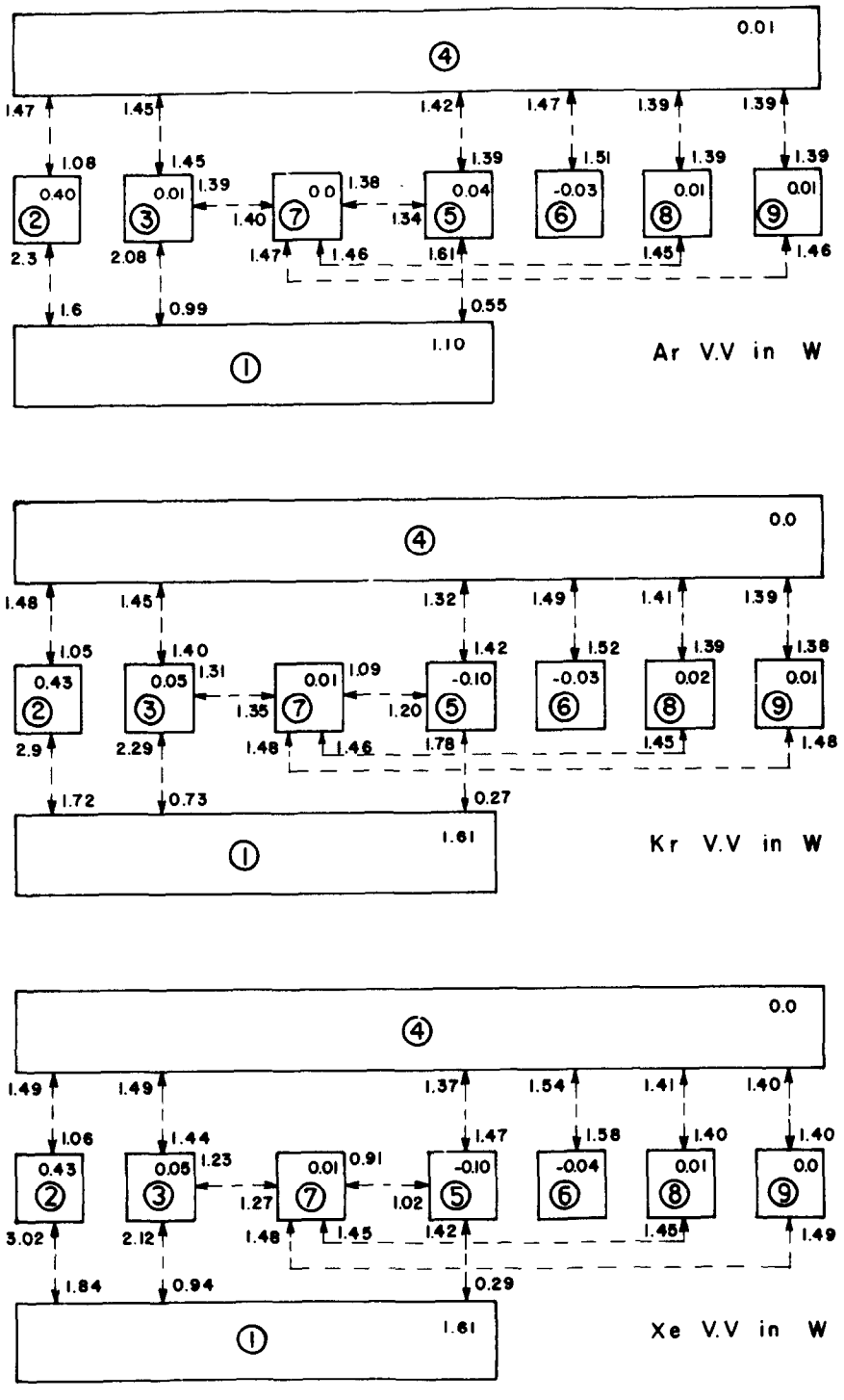

Fig. 1. Transition matrix for vacancy jumps in the vicinity of a noble gas atom in tungsten. The encircled number is the separation in nearest neighbour number. The number in the box is the binding energy of the vacancy to the noble gas atom. The numbers labelling the arrows are activation energies for corresponding transitions.

lar to the transition matrices of a V close to a V or HeV [7], except for the jumps from and towards first and second neighbour positions. Qualitatively the trend of lower vacancy migration energies in a strained crystal agrees well with the calculations of Matthai and Bacon [8]. The binding energy of the vacancy on nth neighbour position to the substitutional noble gas atom is shown in the boxes in the top right corner. From the figure a few details can be learned. Firstly the difference in the transition matrices are only very small. Secondly the migration of a third or fifth neighbour vacancy to a first neighbour position is very much enhanced by the implant. This is easily understood bearing in mind the repulsive force which is exerted by the noble gas atom on the neighbouring W atoms.

3. Monte Carlo calculations

The Monte Carlo approach has been widely used by Fastenau [7] to calculate capture radii for various sink–mobile particle combinations. With this approach the lifetime of a random walker in a box containing a sink in the centre is calculated. Using correct boundary conditions this is equivalent to a random walker in a periodic array of sinks. The average lifetime t_{av} is related to the capture constant Z by comparison with diffusion theory:

$$dc_m/dt = -Kc_m c_s = -Z\nu c_m c_s, \quad (1)$$

c_s is the sink concentration, c_m is the concentration of mobile particles, K is a capture constant which is equal to a trap related capture constant Z times the jump frequency of the mobile particle. Transformation to the number of mobile particles and calculation of the average lifetime gives:

$$t_{av} = 1/Z\nu c_s, \quad (2)$$

where c_s is related to the size of the crystallite used and t_{av} follows from the Monte Carlo calculations. It should be realized that Z as calculated depends on the sink concentration c_s. At lower concentrations Z approaches the value for infinitely low c_s. The crystallite size applied then requires a very long calculation time. Therefore the diffusion theory developed by Ham [9] for spherical traps of constant size arranged on a simple cubic superlattice was applied to derive Z_0 from Z_{c_s}. In ref. [7] this derivation is given and shown to be applicable to this problem.

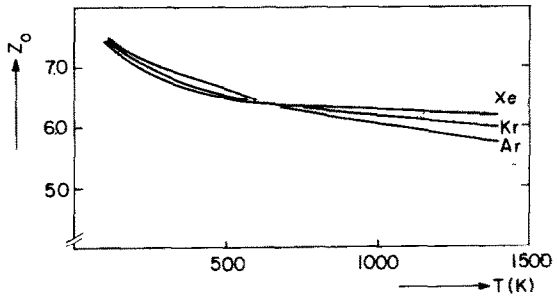

Fig. 2. Low sink concentration limit of the rate constant Z_0 for the vacancy capture by substitutional noble gas atoms in tungsten as a function of temperature.

Table 1
Vacancy trapping probability $P^v(r)$ for different implant–vacancy separations and implants

Implant	Implant–vacancy separation			
	0–2 LU	2–4 LU	4–6 LU	6–8 LU
Ar	0.95	0.51	0.18	0.04
Kr	0.95	0.51	0.19	0.04
Xe	0.96	0.51	0.18	0.04
Perfectly fitting implant	0.58	0.18	0.05	0.01

The vacancy was supposed to be trapped once at a first or second neighbour position. In fig. 2 the thus derived capture constants Z_0 for the different implants are shown. The capture constant for an implant not influencing the near vacancy migration energies is 2.9. It can be seen that at lower temperatures the relative difference in migration energies for different jump directions tends to increase the capture constant Z_0. At higher temperatures Z_0 is smaller but still much larger than the value for non-preferential jump directions.

Trapping probabilities $P^v(r)$ of monovacancies starting from positions within 8 LU from the implant were calculated for stage III temperature (taken here as 550 K). The condition for trapping was the same as mentioned above. A vacancy was supposed to be lost for short-range trapping once outside the sphere of 8 LU. It should be realized that trapping probabilities calculated this way only describe trapping of near vacancies. In those cascades where the vacancy concentration within 8 LU of the implant is quite high, vacancy clustering might occur, thus reducing the trapping probability $P^v(r)$. For implantations with doses $> 5 \times 10^{12}/\text{cm}^2$ cascade overlap will occur. All vacancies escaping short range trapping will increase the vacancy concentration. These vacancies will cluster, escape at the surface or be trapped by an implant, but not necessarily the one initiating its formation. Trapping probabilities for different implant–vacancy separations and implants are shown in table 1 for a temperature of 550 K. Also shown in the table are the data for an implant not exerting strain on the lattice, and thus not influencing the vacancy migration energies.

4. MARLOWE calculations

With the program MARLOWE [3] simulations of 5 keV noble gas implantation on W(100) were performed. It was shown recently that the cut-off radius for vacancy/self-interstitial recombination should be quite large to describe experimentally observed vacancy concentrations. Hou et al. [10] compared MARLOWE calculations with THDS measurements of Mo implanted with 1–3 keV light noble gas atoms. They found that a displacement energy E^d of 33 eV and a cut-off radius of 3.7 LU gave agreement between observed and calculated vacancy concentrations. For W we took E^d 40 eV, the cut-off radius was also taken as 3.7 LU. In fig. 3 results are shown for 5 keV noble gas atoms impinging perpendicularly on the 100 surface, or 10° off the normal. From this figure the trend is clear that the heavier noble gas atoms have a larger fraction of nearby-vacancies than the lighter ones. This can be understood by realizing that energy transfer to lattice atoms is more favourable due to the smaller mass difference between the projectile and target atoms, not only on impinging the surface but also on the final collisions of the implant. By analyzing the individual cascades with respect to the radial vacancy distributions and the calculated trapping probabilities (table 1) the fraction of XV_n formed after annealing to stage III was calculated (XV represents substitutional X). In fig. 4 fractions XV_n for the different projectiles are shown. For Ar a substitutional fraction of 30% is obtained after annealing to stage III. For Kr and Xe substitutional fractions of about 20% were obtained after annealing. It should be realized that since vacancy clustering has been omitted (see sect. 3) trapping probabilities $P^v(r)$ for higher local vacancy concentrations will be overestimated. Thus the fractions XV_n with larger n will be overestimated.

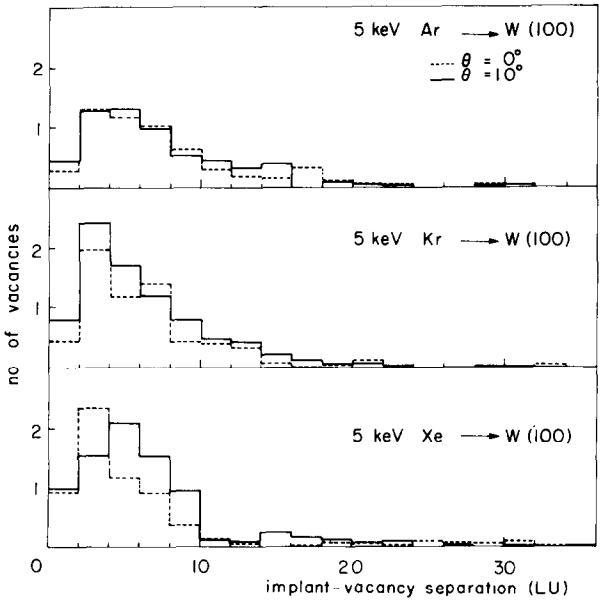

Fig. 3. Radial vacancy distributions for 5 keV noble gas atoms implanted into W(100).

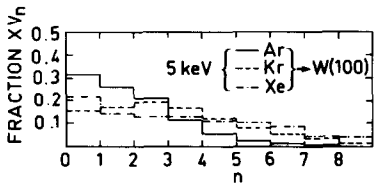

Fig. 4. The fraction XV_n after annealing up to stage III, based on the vacancy distribution for normal incidence and 10° off the 001 channel.

5. Discussion

Several implicit hypotheses were made in the calculations which might influence the results. The trapping probabilities followed from calculated migration energies. Since the migration energies were calculated in a static way with a relaxed lattice the real enhancement of certain jumps may be different, leading to other results. A lower limit for the trapping probabilities is given in table 1.

In the analysis of the MARLOWE results we used the cut-off radius determined for vacancy/self-interstitial recombination as obtained from the experimental vacancy per ion ratio for light ion bombardment. Since the energy transfer to the lattice atoms is higher for heavier ions more vacancies are produced. Effectively the concept of cut-off radius represents a survival probability for vacancies in the vicinity of self-interstitials. Therefore we assume that the value derived by ref. [10] is also valid for the somewhat higher defect concentration in this study.

In the as-implanted samples with THDS virtually no substitutional implants are seen, whereas with Mössbauer and PAC substitutional fractions between 50% and 90% are detected [2,11,12]. We believe that this is caused by the relative "shortsightedness" of the latter methods, whereas with THDS migrating He atoms will be trapped by nearby vacancies. According to MARLOWE calculations there are 1 or 2 vacancies within 2 LU. After annealing to stage III Mössbauer and PAC show substitutional fractions of 10–30%, whereas with THDS a lower fraction is seen. Drainage of He from implants to near vacancies or vacancy-clusters may be the cause.

Finally we would like to comment on the interpretation of the Mössbauer results of refs. [11] and [12]. After implantation of W with 85 keV Xe annealing behaviour

is followed. In the annealing curves different sites are distinguished which we believe to be incorrect for two reasons. After implantation fractions of 40% XeV, 4% XeV_2 and 18% XeV_3 are found. Furthermore the defect they distinguish as XeV_2 disappears after annealing to 100 K above stage III temperature whereas the fraction XeV_3 grows drastically. This is rather unlikely as can be seen from the XeV_n distribution in fig. 4.

We suppose that the so-called XeV_2 is in fact a $XeV_2(2)$, a substitutional Xe atom with a vacancy on second neighbour position, whereas the so-called XeV_3 will be a $XeV_2(1)$, a Xe atom with a first neighbour vacancy. The early disappearance of the $XeV_2(2)$ can be understood by reading the XeV–V transition matrix. A second neighbour vacancy is bound with 0.4 eV, so after annealing till upper stage III a $XeV_2(2)$ will be transferred into a $XeV_2(1)$ either directly or by migration of the vacancy to the fourth neighbour position, and from there across third or fifth to first neighbour position.

We are grateful to Dr M. Hou (Université Libre, Bruxelles, Belgium) for helpful discussions.

This work is part of the research programme of the Stichting voor Fundamenteel Onderzoek der Materie (Foundation for Fundamental Research on Matter) and is supported financially by the Nederlandse Organisatie voor Zuiver Wetenschappelijk Onderzoek (Dutch Organization for the Advancement of Pure Research).

References

[1] A. van Veen, W.Th.M. Buters, G.J. van der Kolk, L.M. Caspers and T.R. Armstrong, Nucl. Instr. and Meth. 194 (1982) 485.
[2] K. Post, F. Pleiter, G.J. van der Kolk, A. van Veen, L.M. Caspers and J.Th.M. de Hosson, Hyp. Interact. 15/16 (1983) 421.
[3] M.T. Robinson and H. Torrens, Phys. Rev. B9 (1974) 5008.
[4] R.A. Johnson and N.D. Wilson, Proc. Int. Conf. Interatomic Potentials and Simulations of Lattice Defects, eds., P.C. Gehlen, J.R. Beeler and R.I. Jaffee (Plenum Press, New York, 1972, p. 301.
[5] K.D. Rasch, R.W. Siegel and H. Schultz, Phil. Mag. A41 (1980) 91.
[6] M. Baskes, private communication.
[7] R.H.J. Fastenau, A. van Veen, P. Penning and L.M. Caspers, Phys. Stat. Sol. (a)47 (1978) 577.
[8] C.C. Matthai and D.J. Bacon, J. Nucl. Mat. 114 (1983) 22.
[9] F.S. Ham, J. Phys. Chem. Sol. 6 (1958) 335; J. Appl. Phys. 30 (1959) 915.
[10] M. Hou, A. van Veen, L.M. Caspers and M.R. Ypma, Nucl. Instr. and Meth. 209/210 (1983) 19.
[11] S.R. Reintsema, E. Verbiest, J. Odeurs and H. Pattyn, J. Phys. F: 9 (1979) 1511.
[12] E. Verbiest, PhD Thesis, Leuven, Belgium (1983).